Membrane–solvent selection for CO2 removal using membrane gas–liquid contactors

Dindore, V.Y.; Brilman, D.W.F.; Geuzebroek, F.H.; Versteeg, G.F.

Published in:
Separation and Purification Technology

DOI:
10.1016/j.seppur.2004.01.014

Publication date:
2004

Available online at www.sciencedirect.com
SCIENCE DIRECT®
Separation and Purification Technology 40 (2004) 133–145
Separation Purification Technology
www.elsevier.com/locate/seppur

Membrane–solvent selection for CO_2 removal using membrane gas–liquid contactors

V.Y. Dindore [a], D.W.F. Brilman [b], F.H. Geuzebroek [c], G.F. Versteeg [a,*]

[a] *Design and Development of Industrial Processes, Faculty of Chemical Technology, University of Twente, P.O. Box 217, 7500 AE Enschede, The Netherlands*
[b] *Sasol Technology Netherlands B.V., Hallenweg 5, 7522 NB Enschede, The Netherlands*
[c] *Shell Global Solutions International B.V., P.O. Box 38000, 1030 BN Amsterdam, The Netherlands*

Received in revised form 21 January 2004; accepted 22 January 2004

Abstract

Membrane gas–liquid contactors can provide very high interfacial area per unit volume, independent regulation of gas and liquid flows and are insensitive to module orientation, which make them very attractive in comparison with conventional equipments for offshore application. However, the membrane adds an additional resistance in the process of mass transfer. The mass transfer resistance of the membrane is affected by the presence of the liquid inside the membrane pores. This wetting of the membrane is determined by the properties of the membrane and the liquid mutually. Hence, a proper choice of the membrane–solvent combination is a critical and determining step in developing membrane gas absorption processes.

Important criteria for the selection of the membrane–solvent combination for membrane gas–liquid contactors, such as the critical entry pressure, contact angle and critical solvent surface tension are evaluated in this paper. These characterizing properties of membranes and solvents are experimentally measured for various membrane and solvent combinations for the case of bulk CO_2 removal. For selected combinations the actual gas–liquid mass transfer process for CO_2 absorption is explored experimentally in the flat sheet as well as in the hollow fiber membrane configuration. The experimental results were compared to the theoretical calculations to determine possible mass transfer limitations due to wetting effects. The polypropylene membrane in combination with propylene carbonate as an absorption liquid was found to be a suitable combination for bulk CO_2 removal using membrane gas–liquid contactors.

Keywords: Membrane contactors; CO_2 removal; Natural gas; Membrane wetting

1. Introduction

The gas absorption using membrane gas–liquid contactors is an emerging technology for selective separation of gaseous components. The microporous membrane used in this process acts as a fixed interface between the gas and the liquid phase without dispersing one phase into another. These membrane gas–liquid contactors offer numerous advantages over conventional mass transfer equipments. The noticeable advantages are operational flexibility, higher volumetric mass transfer rates and easy linear scale up. However, the presence of a membrane adds an additional resistance to the overall mass transfer process in the case of membrane gas–liquid contactors. In the ideal case, the membrane pores are filled with the gaseous component (non-wetted) resulting into negligible mass transfer resistance. However, when the membrane pores are filled with the liquid (wetted), the mass transfer resistance of the membranes becomes significant [1], resulting into economically unviable operation. Thus long-term stable operation of the membrane contactor requires that the pores of the membrane remain completely gas filled (non-wetted) over the prolonged periods of operational time. The wetting tendency of a membrane–solvent combination is mainly determined by properties of the membrane (e.g. pore size), properties of the liquid (e.g. surface tension) and their mutual interactions (e.g. contact angle). In general, liquids with low surface tensions tend to wet the surface more

Abbreviations: *n*-FM, *n*-formyl morpholine; PC, propylene carbonate; PES, polyethersulfone; PP, polypropylene; PS, polysulfone; PTFE, polytetrafluoroethylene

* Corresponding author. Tel.: +31-53-4894337; fax: +31-53-4894774.
E-mail address: g.f.versteeg@utwente.nl (G.F. Versteeg).

1383-5866/$ – see front matter © 2004 Elsevier B.V. All rights reserved.
doi:10.1016/j.seppur.2004.01.014

Nomenclature

A	area (m^2)
C	concentration (mol/m^3)
d	diameter (m)
D	diffusivity (m^2/s)
Gz	Graetz number, vd^2/Dz
J	flux (mol/m^2 s)
k	mass transfer coefficient (m/s)
l	length (m)
m	solubility
P	pressure (Pa)
Q	flow rate (m^3/s)
r	pore radius (m)
R	gas constant
t	time (s)
T	temperature (K)
V	volume of storage vessel (m^3)
x	mole fraction

Greek letters

γ	surface tension (mN/m)
δ	thickness (m)
ϵ	porosity
θ	contact angle
τ	tortuosity

Subscripts and superscripts

c	critical
d	dispersion
eff	effective
G	gas
i	inside
K	Knudsen
L	liquid
m	membrane
o	overall
p	pore
S	solid
w	water
0	initial
∞	final

easily as compared to solvents having higher surface tensions.

The bulk removal of CO_2 is carried out in many gas-based industries such as natural gas, refinery gas or coal gas purification. In addition, the stringent environmental regulations towards the emission of CO_2 have considerably changed the economics of the fossil fueled power plants and energy industries. Absorption in a liquid is the common process used in the industry for CO_2 removal. Most of the solvents used in the bulk removal of CO_2 such as methanol (Rectisol process), propylene carbonate (Fluor solvent), selexol, *n*-formyl morpholine, etc. are organic in nature and have low surface tensions. The 'green' solvent water, on the other hand, has a relatively low solubility. Hence, there is need for reliable guidelines to select the suitable membrane–solvent combination for bulk removal of CO_2. Therefore, the governing and important criteria for the selection of a membrane–solvent combination for the bulk CO_2 removal using membrane gas–liquid contactor are evaluated in the present work. These characterizing properties of membranes and solvents are experimentally measured for various membrane–solvent combinations. For selected membrane–solvent combinations the actual gas–liquid mass transfer process for CO_2 absorption is explored experimentally in the flat sheet as well as in the hollow fiber membrane configuration.

2. Theory

2.1. Mass transfer in the membrane contactor

The mass transfer process in a membrane contactor involves following steps:

1. Transfer of a solute from the bulk gas phase to the membrane surface.
2. Transfer of a solute through the membrane pores to the liquid interface.
3. Transfer of a solute from the liquid interface into the liquid bulk.

Thus the overall mass transfer process consists of three resistances in series: the gaseous phase boundary layer ($1/k_G$), the membrane ($1/k_m$) and the liquid phase boundary layer ($1/k_L$). The overall mass transfer in the gas–liquid membrane contactor can be described with the resistance-in-series model and the overall mass transfer resistance ($1/K_o$) can be obtained by adding the partial resistances in series:

$$\frac{1}{K_o} = \frac{1}{k_G} + \frac{1}{k_m} + \frac{1}{mk_L} \tag{1a}$$

In the case of liquid filled membrane pores, the overall mass transfer resistance is given by Eq. (1b):

$$\frac{1}{K_o} = \frac{1}{k_G} + \frac{1}{mk_m} + \frac{1}{mk_L} \tag{1b}$$

The individual mass transfer coefficient k_G and k_L are mainly determined by the geometry and the flow conditions in membrane contactor and various correlations are available in literature to determine these coefficients [2,3]. The membrane mass transfer resistance is an extra resistance in the membrane gas–liquid contactors. Since convection in the membrane pores can be neglected, the mass transfer resistance of membrane is entirely determined by diffusion of the solute in the membrane pores that are either filled with gas or liquid. The membrane mass transfer resistance of the gas filled

membrane pores can be estimated from Eq. (2) [1]:

$$\frac{1}{k_m} = \frac{\delta}{D_o}\frac{\tau}{\varepsilon} \quad (2)$$

where D_o is the overall diffusion coefficient through the membrane pores and is given by Eq. (3):

$$\frac{1}{D_o} = \frac{1}{D_{ij}} + \frac{1}{D_{Ki}} \quad (3)$$

where D_{ij} and D_{Ki} are diffusion coefficients for molecular and Knudsen diffusion through the membrane pores, respectively. These diffusion coefficients can be estimated using membrane and gas properties [4].

A membrane is wetted when the membrane pores are filled with the liquid phase, in such cases the Knudsen diffusion can be ignored owing to the higher molecular density. In this case the membrane mass transfer resistance is given by Eq. (4) [2]:

$$\frac{1}{k_m} = \frac{\delta}{mD_L}\frac{\tau}{\varepsilon} \quad (4)$$

where D_L is the diffusion coefficient of the solute in the liquid phase. In this mode of operation the solute has to diffuse through the liquid filled pores resulting into a very low membrane mass transfer coefficient. Hence, care must be taken to avoid the filling of membrane pores with the liquid phase.

2.2. Wetting characteristics of membrane–solvent combination

The tendency of the liquid to wet the surface is determined by the surface morphology and properties of the liquid. When a drop of liquid is brought into the contact with a flat polymer surface, the final shape taken by the drop and the wetting of surface depends on the relative magnitudes of the molecular forces that exist within the liquid (cohesive) and between the liquid and the surface (adhesive). These molecular forces and the surface wetting can be predicted from the contact angle made by a liquid drop with the polymer surface. A contact angle of zero results in complete wetting of the porous or non-porous surface, while an angle between 0° and 90° results in spreading of the drop (due to molecular attraction) on a non-porous surface and the wetting of pores on a porous surface. An angle greater than 90° indicates that the liquid tends to bead or shrink away from the solid surface and thus exhibit non-wetting tendencies. The liquids having low surface tension usually wet most polymer surfaces, giving a zero contact angle. However, for the low energy surfaces, like polytetrafluoroethylene (PTFE) and polypropylene (PP), many of the organic liquids having low surface tension found to exhibit non-wetting characteristics [5]. In the case of microporous structures, in addition to the contact angle made by the liquid with the surface, pore size and the surface tension of the liquid are important parameters. For instance, hydrophobic porous membranes do not permit the aqueous liquid to enter into the pores until a certain critical liquid-side overpressure is exerted. This critical entry pressure (CEP) is defined as the trans-membrane pressure difference at which liquid penetrates into the pores of the membrane. The critical entry pressure is correlated to the surface tension of liquid, the contact angle of the liquid on the membrane surface and the size and shape of membrane pores. For the case of sufficiently small uniform cylindrical pores, for which the curvature radius can be assumed to be constant, the critical entry pressure is given by Laplace–Young equation:

$$\Delta P_c = -\frac{2\gamma_L \cos\theta}{r_p} \quad (5)$$

However, most of the membranes do not have cylindrical pores. Some membranes have a fibrous structure and the pores are irregular spaces that remain between adjacent fibers. In other membranes, the pores are holes in a spongy structure and they tend to suffer directional changes and cross linking between them. To take into account such irregular pore structures Franken et al. [6] introduced a geometric coefficient of the pore, B, in the RHS of the Laplace–Young equation; $B = 1$ for cylindrical pores and $0 < B < 1$ for non-cylindrical pores. Kim and Harriott [7] studied the critical entry pressure for liquids in hydrophobic membrane with non-cylindrical pores. They assumed a doughnut type of pore structure and derived an equation similar to the Laplace–Young equation. In which the contact angle θ is replaced by the effective contact angle θ_{eff}. Using this effective contact angle, the mechanical equilibrium state of a membrane–liquid–gas system (as shown in Fig. 1) can be described by the Laplace–Young equation as follows:

$$\gamma_L \cos\theta_{eff} = \gamma_S - \gamma_{SL} \quad (6)$$

where γ is the surface tension, and subscripts L, S, and SL refer to liquid–vapor, solid–vapor and solid–liquid interfaces, respectively. For the polar or hydrogen bonding liquids on the non-polar low energy surfaces, it can be assumed that only van der Waals dispersion forces act between the liquid and solid phase. In this case, the interfacial tension between the solid and liquid phase is given approximately by Eq. (7) [8]:

$$\gamma_{SL} = \gamma_S + \gamma_L - 2\sqrt{\gamma_S^d \gamma_L^d} \quad (7)$$

where γ_S^d and γ_L^d are the dispersion components of surface tension of solid and liquid, respectively. The term $2\sqrt{\gamma_S^d \gamma_L^d}$

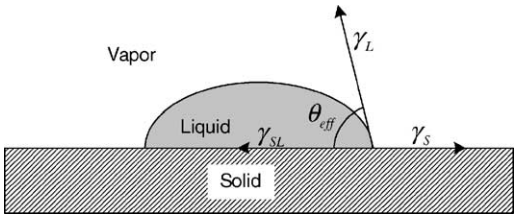

Fig. 1. Contact angle and force balance in wetting of surfaces.

accounts for the dispersion component of the work of adhesion of a liquid to a solid surface. Eqs. (5)–(7) can be used to relate the liquid critical entry pressure with the liquid surface tension:

$$\Delta P_c = \frac{2\left(\gamma_L - 2\sqrt{\gamma_S^d \gamma_L^d}\right)}{r_p} \quad (8)$$

The quantity $\sqrt{\gamma_S^d \gamma_L^d}$ is constant for low surface tension liquids such as high alcohol concentration aqueous solution. For the case of $\gamma_L = 2\sqrt{\gamma_S^d \gamma_L^d}$, the RHS term in Eq. (8) becomes zero and no over pressure is required for wetting of the membrane pores. This value of surface tension is known as the critical surface tension γ_L^c. Thus the critical surface tension is the value of surface tension when critical entry pressure is zero, and can be obtained by the *x*-axis intercept of the critical entry pressure versus surface tension plot. Any solution having a surface tension lower than γ_L^c will therefore spontaneously wet the membrane surface.

In the present study the critical entry pressure and contact angle measurements were carried out for the selected membranes using aqueous ethanol solutions to determine the critical surface tension. The critical entry pressure and contact angle were also measured for the selected membrane–solvent combinations to study the wetting characteristics of the membrane–solvent combinations.

3. Screening of membrane–solvent combinations

Considering the wetting phenomenon as described in Section 2, the selection of a membrane–solvent combination is a very critical step in developing a membrane gas absorption process. A key parameter in the screening of potential solvents is the solubility of CO_2. Table 1 shows the properties and the equilibrium CO_2 solubility in terms of the distribution coefficient for the various commercially available physical solvents. Apart from the solubility, the solvent should be non-toxic, thermally stable, easily regenerable and commercially available at low cost and should have a low vapor pressure to minimize the losses. The solvent should have a low viscosity to avoid high pressure drop over the fiber length. A high solvent viscosity also reduces the mass transfer rates thereby increasing the membrane area requirement. This effect becomes especially noticeable at reduced temperatures. The solvents in Table 1 are commercially available and have proven plant performance for CO_2 absorption processes in conventional contactors and were therefore selected for the initial screening of membrane–solvent combinations. The most important requirements of solvent in membrane gas absorption applications are that the long term use of solvent should not damage the membrane either physically or chemically and that the membrane–solvent combination should have sufficiently high critical entry pressure to avoid wetting.

These solvents were tested with commercially available membranes for mutual compatibility of the membrane–solvent combination. The initial screening of the membrane materials was based on the hydrophobicity of the membrane. Membranes having a high hydrophobicity and low surface energies such as PTFE, polypropylene, PVDF, polysulfone and polyethersulfone were selected. The selected membranes were kept in contact with the solvents over a period of time. These membranes were then carefully investigated for the immediate spreading of a solvent and/or for the damage caused by a solvent to a membrane. Table 2 shows the compatibility of the solvents with the membranes in terms of immediate spreading of the solvent and/or the surface damage of a membrane. As indicated in Table 2 only PTFE and polypropylene membranes were found to be compatible with some of the selected organic solvents. The rest of the membranes showed incompatibility with the selected solvents in terms of morphological damage, swelling, shrinkages, color change or dissolution. Hence, it was therefore decided to use PTFE and polypropylene membranes for further experimental work.

4. Experimental

4.1. Measurement of critical entry pressure and contact angle

As explained previously, the critical entry pressure is of great importance for characterizing the compatibility of a

Table 1
Physical solvents for CO_2 absorption (data for 298 K)

Solvent	CO_2 solubility (m)[a]	Surface tension (mN/m)	Viscosity (cP)	Selectivity CO_2/CH_4	Vapor pressure (Pa)
Propylene carbonate	3.50	41.5	2.5	26.31	11.33
Selexol	3.60	33.5	5.8	14.92	0.097
N-methyl pyrrodilone	4.56	34.4	1.7	13.88	53.33
Dimethyl formamide	4.86	30.2	0.8	–	–
Tributyl phosphate	2.50	27.5	3.4	25.00	–
Glycerol triacetate	3.70	35.8	3.5	20.55	0.13
n-Formyl morpholine	3.15	49.1	6.7	–	869.31
Water	0.82	72.3	1.0	23.5	3167.20

[a] $m = (C_L/C_G)_{equilibrium}$.

Table 2
Membrane–solvent compatibility

Solvent	PTFE	PP	PVDF	PES	PS
Water	✓[a]	✓	✓	✓	✓
Propylene carbonate	✓	✓	×[b]	×	×
Selexol	✓	×	×	×	×
N-methyl pyrrodilone	×	×	×	×	×
Dimethyl formamide	×	×	×	×	×
Tributyl phosphate	×	×	×	×	×
Glycerol triacetate	✓	×	×	×	×
n-Formyl morpholine	✓	✓	×	×	×

[a] Compatible combination.
[b] Incompatible combination.

membrane–solvent combination in a membrane gas absorption process. Eqs. (5) and (8) are indirectly related to the operating temperature since the surface tension of the liquid depends on the temperature. The range of operating trans-membrane pressure, minimum allowable surface tension and hence the operating temperature can be determined from the critical entry pressure and contact angle measurements. In the critical entry pressure measurements only active pores (pores open at both ends of membrane) are taken into account. Since mass transfer in membrane gas absorption takes place through active pores, the critical entry pressure measurement is a good characterization method for the wetting tendency of the membrane–solvent combination in comparison to other methods.

4.2. Materials and methods

Two different experimental techniques were used to measure the wetting characteristics of the membrane–solvent combinations. The critical entry pressure was measured for different membrane–solvent combinations and additionally contact angle measurements were also carried out for the same membrane–solvent combinations. Two types of commercial flat sheet hydrophobic membranes were used; polypropylene (PP) and polytetrafluoroethylene (PTFE). Details of the membranes used in this study are listed in Table 3. Membranes were tested as received without any pretreatment. All solvents used in the study were of analytical grade. Double distilled water was used to prepare the aqueous ethanol solutions with different concentrations.

The experimental setup for critical entry pressure measurement is shown in Fig. 2. It mainly consists of a small stainless steel vessel for holding the membrane and the solvent. A dry membrane was placed in the vessel with support of Teflon gaskets. The solvent was filled into the solvent chamber and pressed into the membrane pores by applying pressure with the help of high-pressure nitrogen fed from a cylinder. The applied pressure was measured with the help of digital pressure transducer. The pressure was gradually increased via a precision pressure regulator till the first drop of the solvent appeared on the membrane surface. This pressure was then defined as the critical entry pressure for the particular membrane–solvent combination.

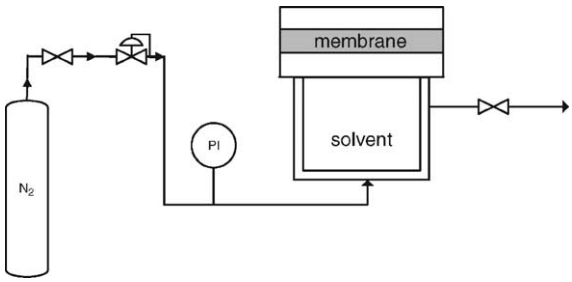

Fig. 2. Experimental setup to measure critical entry pressure.

The contact angles were measured with the sessile drop method using a contact angle measuring instrument (Data Physics, OCA) for aqueous solutions of ethanol and pure solvents on PTFE and PP membranes. A piece of membrane material (of 5 cm × 5 cm) was placed on a platform of the above mentioned measuring device and a 3 μl drop of the solvent was placed on the membrane surface using a micro syringe. The contact angle is calculated using a digital image processor. The average of four to six readings was taken for each individual measurement. All measurements were carried out at room temperature.

Table 3
Membrane characteristics

	Maximum pore size (μm)	Thickness (μm)	Porosity (%)	Inner diameter (μm)	Trade name	Manufacturer
PTFE flat sheet	0.45	158	–	–	TE 36	Schleicher and Schuell
PP flat sheet	0.36	92.5	69	–	PP 1E	Membrana-Accurel
PTFE hollow fiber	1	500	50	1000	Perflon	Sumitomo
PP hollow fiber	0.64	200	∼80	600	Q3/2	Membrana-Accurel

4.3. Measurement of mass transfer characteristics

Experiments were carried out to study the CO_2 absorption using the selected membrane–solvent combinations. Since the mass transfer coefficient is also dependent on the configuration of the contactor, separate experiments were carried out in the flat sheet as well as in the hollow fiber membrane configuration. For each membrane–solvent combination a fresh membrane was used. The experiments are useful to determine the effect of membrane resistance on the overall performance of the process and can indicate the wetting/partial wetting of the membrane.

4.3.1. Experiments with flat sheet membrane configuration

CO_2 absorption experiments were carried out in the flat sheet membrane contactor for the selected solvent and membrane combinations. The experimental setup is shown in Fig. 3. The membrane gas–liquid contactor was a bi-chambered glass vessel with an internal diameter of 8 cm and with a height of 7.5 cm for each compartment. A flat sheet membrane, which is to be tested, separates the two chambers. To minimize gas and liquid side mass transfer resistances, each compartment was equipped with two pitched blade stirrers with the independent stirring motors. The speed of the gas phase stirrers and the liquid stirrers could be varied from 5 to 35 and from 0.25 to 2 rps, respectively. The stirrers in both phases were magnetically driven to avoid the leakage from the contactor. The membranes were glued between metal rings to give an interfacial area of $2.64 \times 10^{-3}\,m^2$. The temperature on the gas and the liquid side was maintained constant using a thermostat water bath. Both compartments were provided with inlet and outlet, to fill and to discharge the fluids. Considering the importance of the trans-membrane pressure on the possible wetting of membrane pores, each compartment was equipped with digital pressure indicator. All experiments were carried out in a batch mode at atmospheric pressure and at 298 K. Before starting the experiment the liquid was thoroughly degassed by applying vacuum. To start the experiments the gas chamber was filled with pure CO_2. As the CO_2 starts absorbing into the solvent, the partial pressure of CO_2 on gas side starts decreasing steadily with time. This drop in the gas side pressure is then noted as a function of time to calculate the absorption flux. The mass balance for CO_2 absorption yields following equation:

$$\ln\left\{\frac{P_{CO_2} - P_{CO_2,\infty}}{P_{CO_{2,0}} - P_{CO_2,\infty}}\right\} = -\frac{mV_L + V_G}{V_L + V_G} K_o A t \tag{9}$$

The slope in a plot of LHS term of Eq. (10) versus time yields the overall mass transfer coefficient, K_o. The experiments were carried out with and without membrane to analyze the effect of the membrane on the overall mass transfer rate.

4.3.2. Experiments with hollow fiber membrane configuration

Absorption experiments were carried out in a single hollow fiber membrane contactor, with absorption liquid flowing through the fiber. Fig. 4 shows schematically the experimental setup used for these absorption experiments. The single hollow fiber membrane contactor used in the experiments was made of glass. The contactor consisted of a jacketed, cylindrical tube with threaded ends. The two ends of a membrane hollow fiber were passed through two small stainless steel (SS) tubes whose inside diameter was slightly larger than the outside diameter of the hollow fiber. The length of the fiber exposed to the gas during the measurements was the distance between these two SS tubes. The distance between the SS tubes was carefully adjusted and the fiber was potted using epoxy resin to the SS tubes on both the ends of the two tubes. The length of the fiber inside the SS tube (>0.07 m) on the liquid entry side provides sufficient distance ($>10d_{in}$) for the laminar liquid flow profile inside the fiber to be fully developed, before it contacts the gas. The hollow fiber between the SS tubes was placed coaxial to the jacketed tube and the two SS tubes were fixed to the ends of the threaded tube without stretching or putting

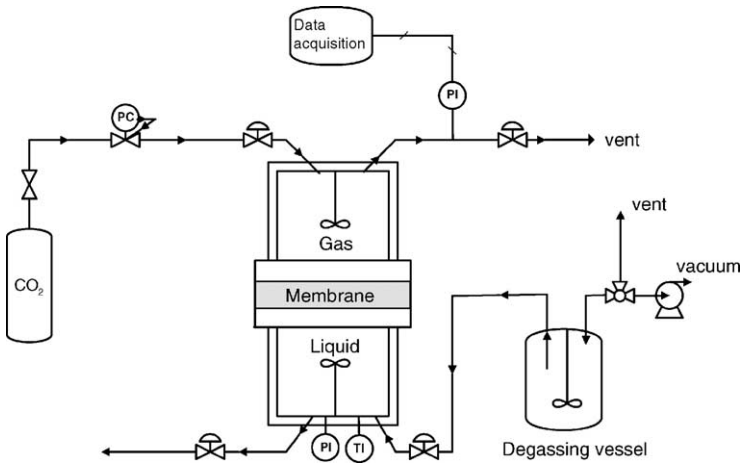

Fig. 3. Measurement of mass transfer flux in flat sheet membrane contactor.

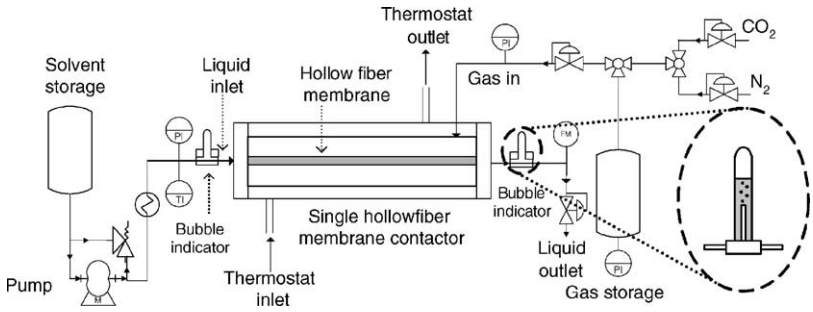

Fig. 4. Measurement of mass transfer flux in hollow fiber membrane contactor.

slack in the fiber. The liquid feed line was connected to the SS tube on the feed side of the contactor. Two vertical glass tubes ('bubble indicators') were attached in the upstream and down stream of liquid feed line so that the possible bubble formation in liquid stream could be observed.

A semi-batch mode of the gas–liquid contacting operation was used during the experiments. The liquid flow through the fiber was continuous. The solvent was fed from a gear pump via a flow controller. The solvent used in the experiments was degassed before usage by applying vacuum in a separate apparatus. The solvent was passed through the heat exchanger to maintain the desired temperature before passing to the single hollow fiber module. The upstream solvent pressure was controlled using a high precision back pressure controller valve. During the experiments sufficient high pressure on the liquid side was maintained to avoid the bubble formation. The CO_2 partial pressure outside the hollow fiber in the contactor was maintained constant by feeding pure CO_2 from a gas supply vessel, through a pressure regulator. From the drop in the pressure of CO_2 in the gas supply vessel, the absorption rate and hence the average CO_2 flux across the membrane was calculated:

$$\langle J \rangle = \left(\frac{V}{RT}\right)\left(\frac{1}{\pi d_i l}\right)\left(\frac{P_1 - P(t)}{t}\right) \tag{10}$$

The theoretical average flux can be calculated by a simple mass balance of CO_2 over the length of fiber:

$$\langle J \rangle = \frac{Q_L m C_G (1 - \exp(-K_o \pi d_i l / Q_L))}{\pi d_i l} \tag{11}$$

The measured flux is then equated to Eq. (11) to calculate the overall mass transfer coefficient K_o.

5. Results and discussion

5.1. Measurement of critical entry pressure

To study the effect of surface tension the critical entry pressure experiments were carried out ambient temperature (≈293 K) for flat sheet membranes. Fig. 5 shows the critical entry pressure for the flat sheet membranes for various concentrations of aqueous ethanol. Only four points could be measured with PP flat sheet membrane. Because of the lower mechanical strength and low burst pressure (0.9 bar) of the membrane, it was not possible to measure the critical entry pressure for lower concentrations of ethanol. Moreover, at higher ethanol concentrations of the ethanol the membrane wetted spontaneously.

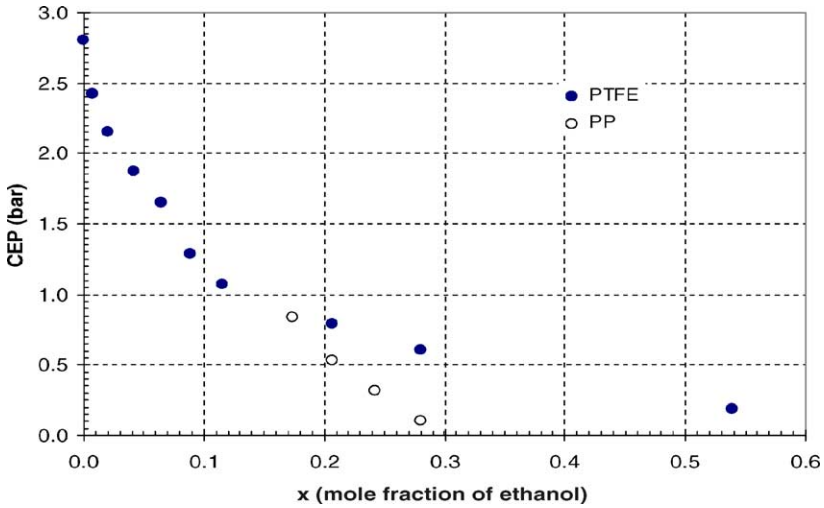

Fig. 5. Critical entry pressure for aqueous ethanol solutions.

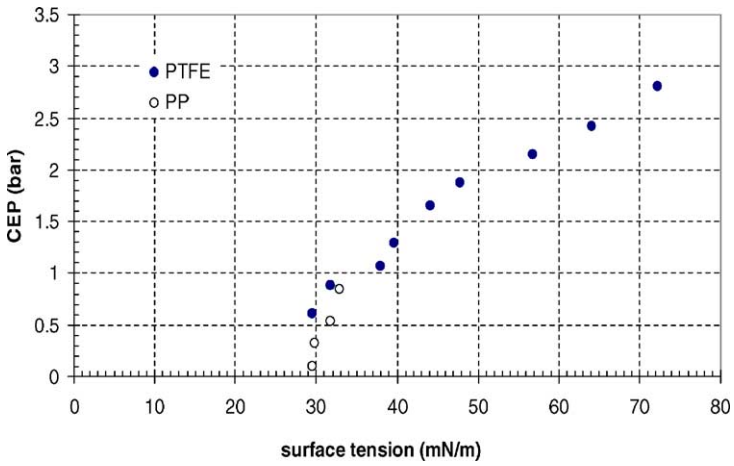

Fig. 6. Effect of surface tension on entry pressure.

The effect of the surface tension on the critical entry pressure is shown in Fig. 6. The critical entry pressure shows linear dependence on the surface tension at relatively low surface tension values (i.e. at high ethanol concentrations). However, for the higher surface tension liquids, the experimental data recede below the linear dependency in the case of PTFE membrane. This is because at lower concentrations of the ethanol, the dispersion component of the surface tension, $\sqrt{\gamma_S^d \gamma_L^d}$, is not constant and depends on the ethanol concentration. In such cases the linear dependence of critical entry pressure on surface tension is no longer valid. The critical surface tension, γ_L^c, for the given membrane can be calculated from the *x*-intercept of the plot. Thus determined values of the critical surface tension for PP and PTFE membrane are 29 and 20 mN/m, respectively. These values are in good agreement with the literature data of 29 and 18 mN/m for PP and PTFE materials, respectively [5]. Since any liquid having surface tension lower than the critical surface tension wets the membrane spontaneously, the solvents to be used must have a substantially higher surface tension than the critical surface tension values. Among the selected solvents besides water only propylene carbonate, *n*-formyl morpholine and glycerol triacetate have sufficiently high surface tensions and are compatible with both PTFE and PP membranes. The critical entry pressure values for these solvents are determined using flat sheet membranes and are presented in Table 4. The critical entry pressure for the water–PP and the *n*-formyl morpholine–PP combinations could not be determined because of the lower burst pressure of the PP membrane.

Table 4
Critical entry pressure for selected solvents

Solvent	Critical entry pressure (kPa)	
	PTFE	PP
Water	310	>90
Propylene carbonate	110	78
n-Formyl morpholine	130	>90
Glycerol triacetate	53	7.5

5.2. Measurement of contact angle

Contact angles of distilled water and aqueous solutions of the ethanol on PTFE and PP membranes were measured at ambient conditions. The measured contact angles are summarized in Table 5. The results indicate that the contact angle θ decreases with increasing the ethanol concentration. To analyze the effect of ethanol concentration on the contact angle, cosine of angle θ is plotted as a function of ethanol mole fraction in Fig. 7. The plots of the contact angle versus ethanol mole fraction are fitted to best fit empirical equation of type:

$$\cos\theta = \cos\theta_w + \frac{ax}{1+bx} \tag{12}$$

where a and b are fitting parameters and x is the alcohol concentration in mole fraction. $\cos\theta_w$ represents the contact angle of pure water on the membrane surface. As seen in Fig. 7, excellent fits were achieved, with correlation coefficients greater than 0.995. The values of experimentally obtained $\cos\theta_w$ and empirically fitted $\cos\theta_w$ demonstrate a good agreement. Fig. 8 shows the plot of the cosine of the contact angle θ versus the surface tension. In general a rectilinear relation can be seen between $\cos\theta$ and surface tension for PTFE membrane, a similar trend is reported in the literature [5] for various liquids and hydrophobic surfaces. For PP membrane two distinct trend lines can be observed. The points below $\cos\theta = 0.0$ fall on the line, which has approximately the same slope as that of PTFE line. However, the points above $\cos\theta = 0.0$ can be correlated with a line that has higher slope, indicating that a small decrease in the surface tension results in a substantial decrease in the contact angle. This can be attributed to the porous structure of the membrane. The membranes used in this work do not have ideally smooth surfaces. The roughness is caused by the presence of the pores, so the liquid droplets are in con-

Table 5
Contact angle for various membrane–solvent combinations (293 K)

Membrane	Liquid	Ethanol concentration (vol.%)	γ (mN/m)	θ (°)
Polypropylene	Distilled water	–	72.30	117.70
	Ethanol–water	2	64.18	106.88
		5	56.84	103.80
		10	47.80	94.49
		20	39.70	81.60
		30	34.33	71.15
		40	31.80	60.53
	Propylene carbonate	–	42.00	90.83
	n-Formyl morpholine	–	48.14	94.56
PTFE	Distilled water	–	72.30	127.42
	Ethanol–water	2	64.18	122.10
		5	56.84	115.11
		10	47.80	110.39
		20	39.70	103.79
		30	34.33	98.01
		40	31.80	95.90
	Propylene carbonate	–	42.00	106.40
	n-Formyl morpholine	–	48.14	110.80

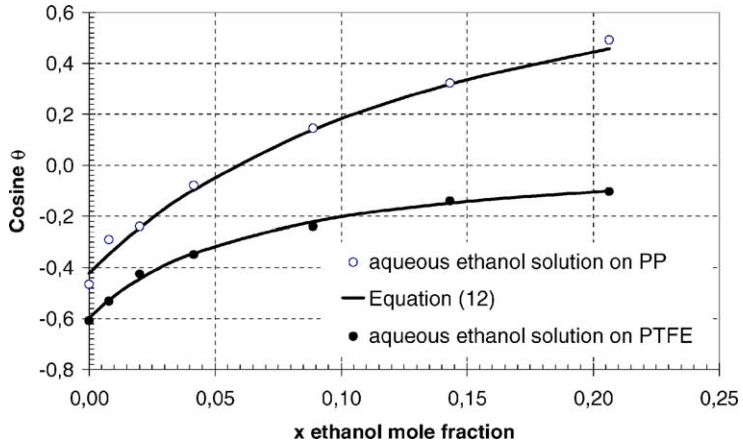

Fig. 7. Contact angle measurements for aqueous ethanol solutions.

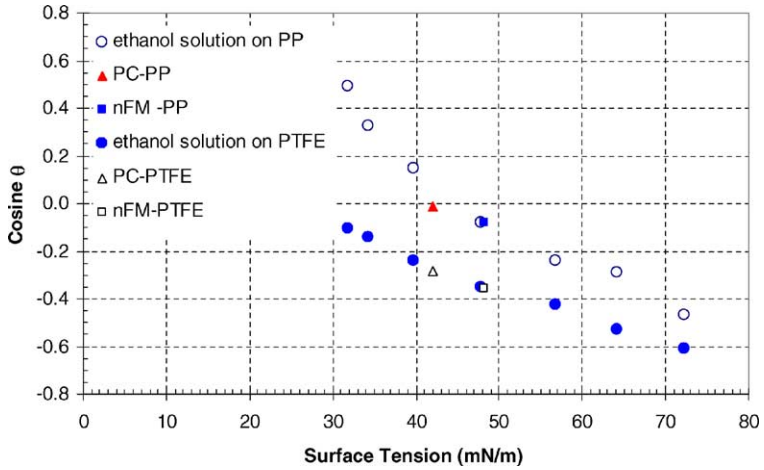

Fig. 8. Effect of surface tension on contact angle.

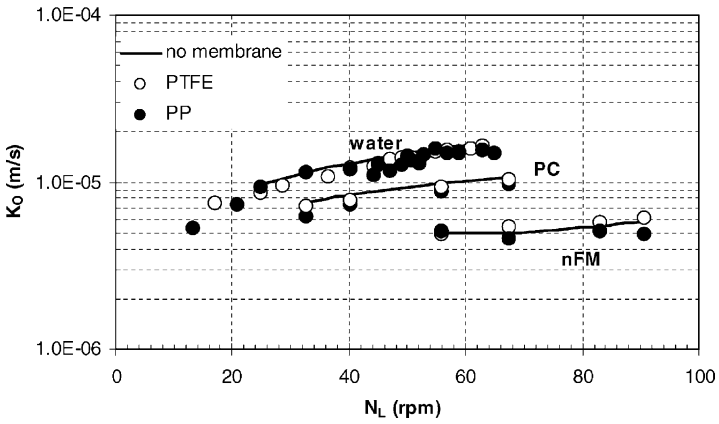

Fig. 9. Mass transfer coefficient in flat sheet membrane contactor.

tact with both the rough polymer surface as well as the air cavities. For such a system, the apparent effective contact angle is always higher than the true intrinsic contact angle on the clean polished surface when the latter greater than 90°, and the apparent effective contact angle is always smaller than the true intrinsic contact angle on the clean polished surface if the true intrinsic contact angle is lower than 90° [5]. Thus apparent contact angle in case of PP membrane decreases sharply below $\cos\theta = 0.0$ or $\theta = 90°$. On the other hand, for example the contact angle of pure water on a smooth PTFE surface reported in the literature varied from 108° to 112° [9], whereas in this work the contact angle reached a value of 127°, indicating that surface roughness resulted into increased apparent contact angle. It is interesting to note that the contact angles for propylene carbonate and *n*-formyl morpholine also fall close to the straight line determined for both membranes using the aqueous ethanol solutions.

5.3. Measurement of mass transfer flux using flat sheet membranes

To study whether the mass transfer resistance in the liquid phase was influencing the absorption process, the mass transfer resistance in the liquid phase was measured with absorption of CO_2 in the various solvents. Pure CO_2 and a high stirrer speed on the gas side were used in the absorption experiments in order to eliminate the gas side mass transfer resistance. The experiments were carried out with and without membrane to analyze the effect of the membrane on the overall mass transfer rate. The results are presented in Fig. 9. Although in the presence of membrane the gas–liquid interface is fixed ('no-slip' boundary) and in the absence of membrane the gas–liquid interface can be freely moving ('free-slip' boundary), from Fig. 9 it can be concluded that the presence of the membrane does not influence the overall mass transfer coefficient. It can also be concluded that the membranes used in these experiments are not wetted by the solvents. Moreover, it appears that the active mass transfer area in both cases is same and the non-porous part of the membrane does not affect the overall mass transfer process. In the experiments without membrane, the liquid stirrer speed could not be chosen above 90 rpm because the flat interface was then disturbed by the stirrer movement. A flat, smooth, horizontal gas–liquid interface is essential to calculate the exact gas–liquid interfacial area and absorption flux. On the other hand, the presence of membrane offers the possibility to increase the stirrer speed, thus higher k_L,

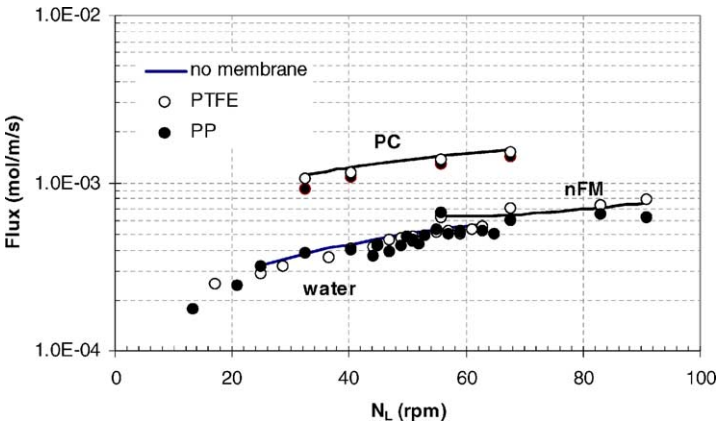

Fig. 10. Mass transfer flux in flat sheet membrane contactor.

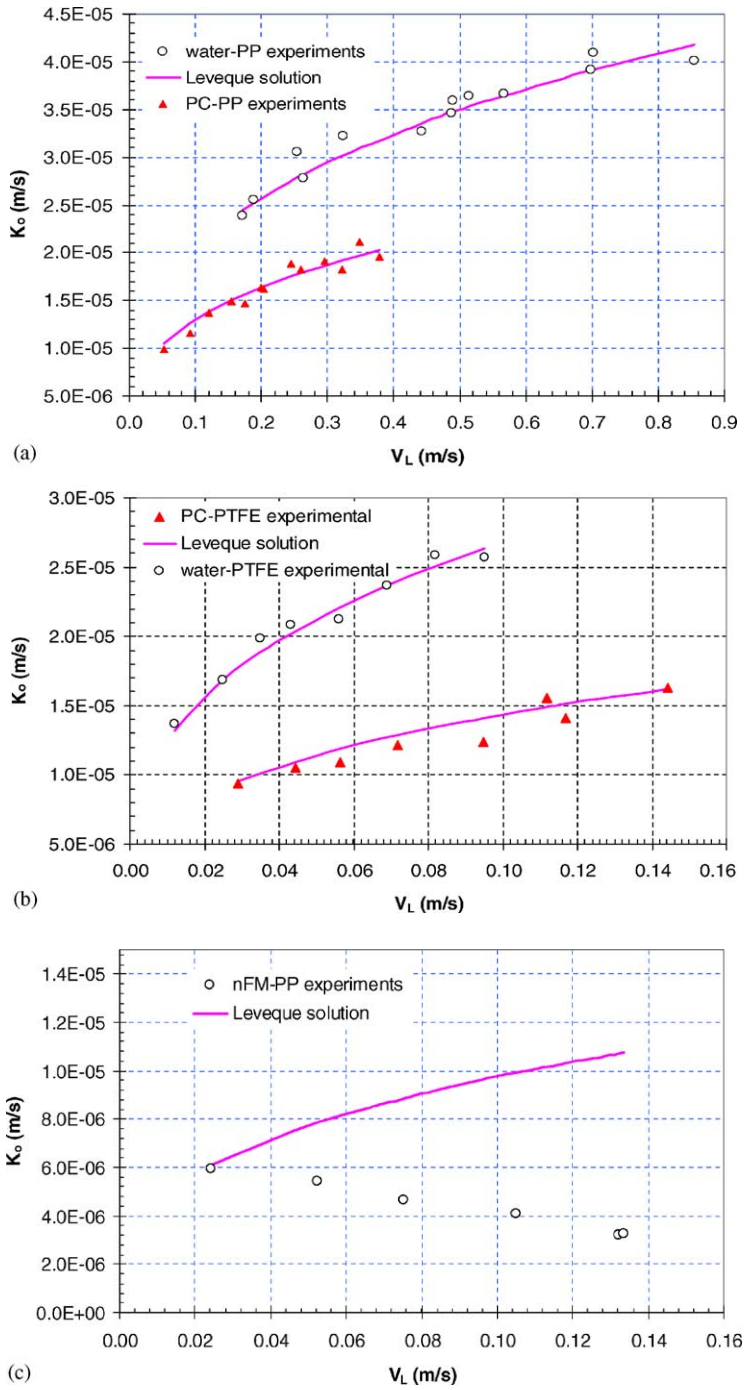

Fig. 11. (a) Mass transfer coefficient in PP hollow fiber membrane contactor. (b) Mass transfer coefficient in PTFE hollow fiber membrane contactor. (c) Mass transfer coefficient in PP hollow fiber membrane contactor using *n*-FM as an absorption liquid.

without disturbing the interfacial area. This can be useful if higher mass transfer coefficients are required, e.g. in the determination of kinetic data. Fig. 9 also indicates that, the overall mass transfer coefficient is a strong function of the liquid side stirrer speed. This indicates that the liquid side mass transfer resistance is the controlling parameter in the overall mass transfer process. The overall mass transfer obtained for the different solvents is in line with the viscosity of the solvents, i.e. a solvent having a higher viscosity (i.e. *n*-FM) demonstrate a lower mass transfer coefficients and vice versa.

Fig. 10 shows the measured CO_2 flux as a function of the liquid stirrer speed. Note that the flux obtained for the water is lower as compared to propylene carbonate and *n*-formyl morpholine solvents, due to the lower solubility of CO_2 in water. Amongst the solvents used in the experiments, propylene carbonate seems to have the highest mass transfer flux and moderate overall mass transfer coefficient.

5.4. Measurement of mass transfer flux in a single hollow fiber membrane module

CO_2 absorption experiments were carried out in a single hollow fiber membrane module using two different hollow fibers (PTFE and PP) and three different solvents. The details of the hollow fiber membranes used in the experiments are given in Table 3. In order to minimize the gas side mass transfer resistance experiments were carried out using pure CO_2 on the shell side. The experiments were carried out at atmospheric pressures and at 293 K. Several correlations have been developed by many investigators to predict the mass transfer coefficient in a hollow fiber membrane contactor for both fiber and shell side flow. However, all the published work is limited to aqueous solvents in the case of gas–liquid applications. Two asymptotic correlations based on the heat transfer analogy of Graetz–Leveque equations are widely used to predict the mass transfer coefficient on the fiber side [3,10].

$$Sh = 1.62(Gz)^{1/3}, \quad Gz > 20 \tag{13a}$$

$$Sh = 3.67, \quad Gz < 10 \tag{13b}$$

Eq. (13a) is the well-known Leveque solution, a limiting case of the more general Graetz solution. Eq. (13a) is valid for the entrance region where the concentration profile has still to build up, $Gz > 20$, whereas Eq. (13b) is applicable for long fibers where the concentration profile is completely developed, $Gz < 10$.

Fig. 11a and b shows the effect of the liquid velocity on the overall mass transfer coefficient for PP and PTFE membranes with water and propylene carbonate, respectively. It is clear from these figures that the fiber mass transfer coefficient can be described well with Eq. (13a) and that therefore the controlling resistance to mass transfer process is indeed in the liquid phase. Moreover, the Leveque equation can also be used to predict the fiber side mass transfer coefficient in the case of gas absorption using organic solvents. Within the time frame of experiments, no decrease in the absorption flux due to aging of the fiber was observed.

Experiments were also carried out using polypropylene–*n*-FM as a membrane–solvent combination. The results are given in Fig. 11c. As shown in this figure, the mass transfer coefficient obtained in this case is very low. Now, the overall mass transfer coefficient even decreases with increasing the liquid velocity. These results can be explained by partial wetting of the membrane. The pressure drop of the liquid inside the fiber lumen increases with the liquid velocity and the fiber length according to the Hagen–Poiseuille law. Since *n*-FM has a high viscosity as compared to water and propylene carbonate, this pressure drop over the fiber in the case of *n*-FM is significant leading to membrane wetting in the initial part of the fiber. This phenomenon was observed visually by the presence of liquid droplets at the outer surface of the membrane, especially near the inlet of the fiber. As the length of the wetted portion increases with increase in the liquid velocity, the average mass transfer coefficient over the length of fiber decreases with the liquid velocity. Thus a pressure drop over the membrane fiber is also a critical parameter for non-wetted mode of operation. Similar results were obtained for the *n*-FM and PTFE combination.

6. Conclusion

Important criteria, such as critical entry pressure, critical surface tension of the membrane and contact angle, in the selection of the membrane–solvent combination for the development of membrane gas absorption have been investigated. These criteria are evaluated for the case of bulk CO_2 removal using physical organic solvents. Based on these criteria a selection of mutually compatible membrane–solvent combinations for this application has been performed. The measurement of 'critical entry pressure' and 'critical surface tension' is a simple experimental method to select a suitable membrane–solvent combination for a membrane gas absorption process. The critical entry pressure and critical surface tension are also useful in determining the operating conditions such as allowable solvent surface tension, temperature and trans-membrane pressure. The experimentally determined values of critical surface tension for PTFE and PP micro-porous membrane are in good agreement with literature values of homogeneous non-porous PTFE and PP materials, indicating that critical surface tension is independent of the porous or non-porous structure of the material.

The measurement of the contact angle indicates that contact angles decrease with alcohol concentration and hence with the surface tension of the liquid. In general, straight line relation between the cosine of angle, θ, and liquid surface tension is observed even for the liquids having different chemical structure. The porous structure of the membrane causes an increase in the apparent contact angle when the intrinsic true contact angle on non-porous cleaned polish surface is more than 90°.

For the selected membrane–solvent combinations, the membrane mass transfer resistance is found to be negligible in the non-wetted mode of operation. The fiber side mass transfer coefficient in the case of organic solvent can be predicted using Leveque equation. A high pressure drop over the fiber length may lead to (partial) wetting in the initial part of the fiber and hence in such cases low mass transfer rates are observed. For each membrane–solvent combination a fresh membrane was used and within the time frame of experiments no significant decrease of mass transfer flux due to aging of membranes was observed.

PTFE and polypropylene membranes in combination with propylene carbonate seem to be promising candidates for the absorption of CO_2 in a membrane gas absorption process. Looking at the cost and the manufacturing difficulties in PTFE micro-hollow fibers, a polypropylene membrane in combination with propylene carbonate as CO_2 absorption liquid seems to be the best choice among the tested

membrane and solvent combinations and will therefore be used in further studies.

Acknowledgements

This research is part of the research program performed within the Centre for Separation Technology (CST), which is a co-operation between The Netherlands Organization for Applied Scientific Research (TNO) and the University of Twente. We acknowledge Herman Bruns for his assistance to the experimental work and Wim Leppink and Benno Knaken for the construction of the experimental setup.

References

[1] H. Kreulen, C.A. Smolders, G.F. Versteeg, W.P.M. van Swaaij, Determination of mass transfer rates in wetted and non-wetted microporous membranes, Chem. Eng. Sci. 48 (1993) 2093–2102.

[2] E.L. Cussler, B.W. Reed, M.J. Semmens, Membrane contactors, in: R.D. Noble, S.A. Stern (Eds.), Membrane Separation Technology: Principles and Applications, Elsevier, Amsterdam, 1995, pp. 467–490.

[3] M.C. Yang, E.L. Cussler, Designing hollow-fiber contactors, AIChE J. 32 (1986) 1910–1915.

[4] E.A. Mason, A.P. Malinauskas, Gas transport in porous media: the dusty gas model, Chem. Eng. Monograph 17, Elsevier, Amsterdam, 1983.

[5] W.A. Zisman, Relation of the equilibrium contact angle to liquid solid constitution, in: R.F. Gould (Ed.), Contact Angle Wettability and Adhesion, American Chemical Society, 1964, pp. 1–51.

[6] A.C.M. Franken, J.A.M. Nolten, M.H.V. Mulder, D. Bargeman, C.A. Smolders, Wetting criteria for the application of membrane distillation, J. Membr. Sci. 33 (1987) 315–328.

[7] B. Kim, P. Harriott, Critical entry pressure for liquids in hydrophobic membranes, J. Colloid Interface Sci. 115 (1) (1987) 1–8.

[8] D. Bargeman, F. van Voorst Vader, Effect of surfactants on contact angles at non-polar solids, J. Colloid Interface Sci. 42 (1973) 467–472.

[9] J. Drelich, J. Miller, R.J. Good, The effect of drop (bubble) size on advancing and receding contact angles for heterogeneous and rough solid surfaces as observed with sessile-drop and captive-bubble techniques, J. Colloid Interface Sci. 179 (1) (1996) 37–50.

[10] H. Kreulen, C.A. Smolders, G.F. Versteeg, W.P.M. van Swaaij, Microporous hollow fiber membrane modules a gas–liquid contactor. Part 1. Physical mass transfer processes, J. Membr. Sci. 78 (1993) 197–216.